Monitoring of near surface gas seepage from a shallow injection experiment at the CO_2 Field Lab, Norway

D.G. Jones [a],[*], A.K.A.P. Barkwith [a], S. Hannis [a], T.R. Lister [a], F. Gal [b], S. Graziani [c], S.E. Beaubien [c], D. Widory [b],[1]

[a] British Geological Survey, Environmental Science Centre, Keyworth, Nottingham NG12 5GG, UK
[b] Bureau de Recherche Géologique et Minière, 3 Avenue Claude Guillemin, BP 36009, 45060 Orleans, Cedex 2, France
[c] Università di Roma "La Sapienza", Dip. Scienze della Terra, P.le A. Moro 5, 00185 Roma, Italy

ABSTRACT

Near surface gas measurements are presented from a shallow (20 m depth) CO_2 injection experiment at the CO_2 Field Lab site in Svelvik, Norway, which was designed to test a variety of monitoring tools. Small areas of surface seepage of CO_2 were detected during the experiment and these spread as the injection rate was increased. These features only accounted for a small fraction of the injected gas. Isotopic measurements revealed traces of injected CO_2 at 50 cm depth nearer the injection point. The spatial extent of this is unknown but it is not likely to imply a significant amount of CO_2 seepage. The locations of the gas escape were not as anticipated by prior modelling and highlight the difficulty of predicting where leakage may occur and, hence, where to deploy monitoring equipment. This unpredictability and the limited size of the seeps implies that monitoring will have to be flexible, preferably mobile and capable of detecting small features in large areas if successful leakage detection at surface is to be achieved. Low level seepage, such as that suggested isotopically here, could be significant for carbon auditing if it occurs over wide areas. This could be tested in areas of natural CO_2 seepage.

© 2014 The Authors. Published by Elsevier Ltd. This is an open access article under the CC BY license (http://creativecommons.org/licenses/by/3.0/).

1. Introduction

Carbon capture and storage (CCS) is considered to be an important part of the lowest cost solution for achieving greenhouse gas emissions reduction targets (International Energy Agency, 2009). A large number of projects will be needed worldwide if these targets are to be met. Whilst a carefully selected and well managed geological CO_2 storage site is not expected to leak, the possibility needs to be considered, and leakage detection monitoring is required by legislation, such as the EU Directive on Geological Storage of CO_2 (European Union, 2009b). Should any leakage occur, then the amendment to the European Emissions Trading Scheme (European Union, 2009a) requires that it is quantified.

Monitoring techniques have been tested at sites across the world at different scales. However, protocols for leakage detection are not yet mature and further testing is required to define the sensitivities of a range of techniques to detect migration and leakage of CO_2 in the near surface environment. The CO_2 Field Lab project (Bakk et al., 2012; Dillen et al., 2009) aimed to assess monitoring systems using controlled CO_2 injection experiments at its site near Svelvik in Norway. The aim of the first stage of the project was to inject CO_2 in a shallow, 20 m deep, 45° inclined borehole and to apply a range of monitoring methods to track the subsurface movement of the CO_2 and its eventual leakage to the atmosphere. This shallow experiment was intended as a precursor to a deeper injection. It provided an opportunity to test various monitoring methods (e.g. geophysics, hydrogeochemistry, surface gas) at the site, with a view to studying the impact of the vadose zone on the measurements. The shallow experiment also provided an opportunity to rehearse and coordinate all surface monitoring methods before they are applied to the monitoring of a deeper injection. The deeper experiment would also allow additional techniques to be assessed, such as seismic, to visualise the CO_2 distribution underground.

2. Background

The experimental site is on the Svelvik Ridge about 50 km south of Oslo (Fig. 1). It occupies a non-active part of a sand and gravel

* Corresponding author. Tel.: +44 115 936 3576; fax: +44 115 936 3576.
E-mail addresses: dgj@bgs.ac.uk (D.G. Jones), andr3@bgs.ac.uk (A.K.A.P. Barkwith), sann@bgs.ac.uk (S. Hannis), trl@bgs.ac.uk (T.R. Lister), f.gal@brgm.fr (F. Gal), stefano.graziani@uniroma1.it (S. Graziani), stanley.beaubien@uniroma1.it (S.E. Beaubien), widory.david@uqam.ca (D. Widory).
[1] Present address: UQAM/GEOTOP, Earth and Atmosphere Sciences Department, Montréal H3C 3P8, Canada.

Fig. 1. Location of the CO_2 Field Lab site at Svelvik.

Fig. 2. Injection rates measured using flow rates and pressures at the well head during the shallow experiment.

quarry, which is located in a glaciofluvial-glaciomarine terminal deposit formed during the Ski stage of the Holocene deglaciation (Sørensen, 1981). The ridge extends across Drammensfjord and reaches a height of 70 m above sea level (See Figure 1 in Barrio et al., in press and Figure 3 in Dillen et al., 2009), although the shallow experiment was on a flat area at an elevation of no more than about 5 m above sea level. The chosen site comprises cross bedded and southerly dipping sediments in the top 9 m, based on Ground Penetrating Radar data, and NNW-SSE reflectors below 20 m depth, seen on 2D seismic sections. The laminated and channelled nature of the sediments was apparent in post-experimental sampling, with grain sizes ranging from coarse sand to cobbles and similar to the sediments visible in near vertical exposures higher up the ridge. Coarse sand free of pebbles was recovered below 19 m, just above the injection depth of 20 m.

The CO_2 was injected through a well drilled at 45° inclination to a target depth of 20 m, with the well head and injection equipment located 20 m to the east of the injection point. From the 7th to 12th September 2011, 1.7 tonnes of CO_2 were injected with a well head pressure of 1.9–2 bar. The injection of CO_2 was continuous, however the rate was increased in four incremental stages from 5 kg per hour up to 17.5 kg per hour (Fig. 2). The shallow subsurface was monitored using a combination of geochemical and geophysical techniques, including downhole geophysical and geochemical monitoring and surface gas and bacterial activity monitoring (Barrio et al., in press; Gal et al., 2013). The water table was at about 1 m depth, although this fluctuated by up to 20 cm in the area around the injection point during the experiment. Below about 12–15 m the groundwater passed generally from fresh to saline water of near seawater composition.

This paper presents the results of near surface gas monitoring associated with the shallow injection experiment carried out by the British Geological Survey (BGS) and the Bureau de Recherche Géologique et Minière (BRGM) with collaboration on continuous soil gas monitoring from the University of Rome 'La Sapienza'. An overview of the whole experiment is provided elsewhere (Barrio et al., in press) and the hydrochemical results have also been reported (Gal et al., 2013).
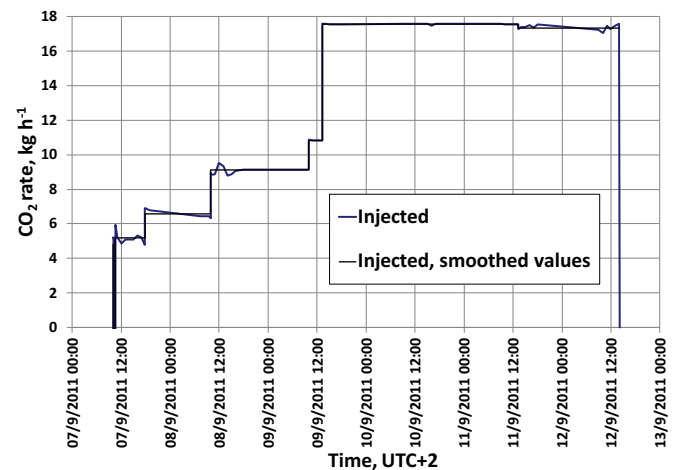
3. Materials and methods

Measurements included near surface gas concentrations, CO_2 fluxes across the ground surface into the atmosphere, concentrations (and calculated flux rates) in the near ground atmosphere and isotope measurements both in groundwater and surface gas. Continuous measurements were made at a relatively small number of locations and areal coverage was achieved by point measurements at periodic intervals.

Soil gas samples were collected by one of two methods. Firstly, BGS used a probe consisting of an 8 mm diameter (4 mm ID) stainless-steel tube onto which two solid steel cylinders were welded to act as pounding surfaces when installing and removing the probe with a co-axial hammer. Prior to insertion, a sacrificial tip was fitted to the bottom of the probe to prevent blockage. The probes were inserted to a depth of 50 cm. This is shallower than the normal depth for such measurements (80–90 cm) but the greatest that could be achieved across the site consistently because of the abundant pebbles and larger clasts within the sediments. In situ soil gas measurements of CO_2, H_2S, CH_4, and O_2 concentrations were made using a Draeger X-am 7000 or a Geotechnical Instruments GA2000 portable gas analyser. ^{222}Rn (radon) and ^{220}Rn (thoron) were measured via the soil gas probes using a Pylon AB5 radon monitor. Since the measurement grid was marked out it was possible to re-occupy the same sample points exactly or within a few centimetres.

In addition, soil gas concentrations were assessed daily by BRGM (also at 50 cm depth) through permanently installed 1 m long copper sampling tubes, installed into a drilled hole, using another portable infra-red gas analyser (LFG20). CO_2 and O_2 were directly evaluated in the field and an additional sample was collected in a glass scintillation flask to determine ^{222}Rn activities later that day (3–6 h after sampling) using an Algade CALEN alpha counting system. As background CO_2 concentrations in the soil were often close to atmospheric levels, more accurate CO_2 (and O_2, N_2 and Ar) data were obtained by collecting samples in Tedlar bags and analysing the gas 1–2 h after sampling in a field laboratory using a portable gas chromatograph (Agilent 3000A microchromatograph). A small number of samples were later analysed by laboratory gas chromatography to check the field values and to provide C isotope data.

In collaboration with the University of Rome "La Sapienza", a Gas Probe ("GasPro") monitoring station was installed by BGS to continuously measure the concentration of CO_2, temperature and atmospheric pressure at three separate points using probes buried

at 50 cm depth. Continuous records were also obtained by BRGM from two Barasol ^{222}Rn probes and from a CO_2/O_2 probe (Gasclam) installed in boreholes at 50 cm depth. CO_2 concentrations and carbon (δ^{13}C) and oxygen (δ^{18}O) isotope composition of CO_2 gas were measured continuously 50 cm above the water table using an Aerodyne Quantum Cascade laser instrument.

CO_2 flux measurements were taken by BGS using a West Systems portable flux metre with a LICOR LI-820 IR detector connected via Bluetooth to a Trimble Juno or Acer n300 palm-top computer (PDA) with built-in GPS. Measurements took 1–3 min depending on the soil flux rate. Flux was normally measured before soil gas adjacent to the soil gas points. A continuous flux monitoring station was also installed by BGS at the site, consisting of a Licor Li-8100 system with a Li-8150 multiplexer and four accumulation chambers controlled by the Licor automated operating and data-logging system.

Flux was also determined by BGS using the eddy covariance (EC) method. A Campbell Scientific EC system, mounted on a tripod at a height of 2 m, measured 3D wind parameters and CO_2 concentration, air temperature, pressure and relative humidity at 10 Hz. The data were post-processed using the software tool EdiRe (Edinburgh University, 2011), which produces a range of corrected means, deviations and fluxes after a number of de-spiking, filtering and correction processes. Data were, in general, computed for 30-min intervals.

Atmospheric CO_2 concentrations were measured by BGS with a Boreal Laser open-path laser CO_2 probe linked to a GasFinder FC analyser. Data were collected every second using Boreal GasMap software with positions from either a Pharos or Trimble ProXT GPS receiver. The laser system was deployed mainly in static mode, at different locations, with the probe measuring only a few cm above the ground surface. The equipment was tested briefly in mobile mode by hand carrying the system around the site, but mobile operation was difficult because of the profusion of other monitoring equipment deployed at the site.

In addition to the meteorological parameters obtained with the EC system, supplementary data were gathered by BGS with a LaCrosse WS2801-IT weather station set up on the portacabin on the site; sensors mounted on the roof gave averaged hourly readings of temperature, pressure, relative humidity, wind speed and direction and rainfall.

As well as surface gas measurements, BRGM was also responsible for most of the groundwater monitoring, the results of which
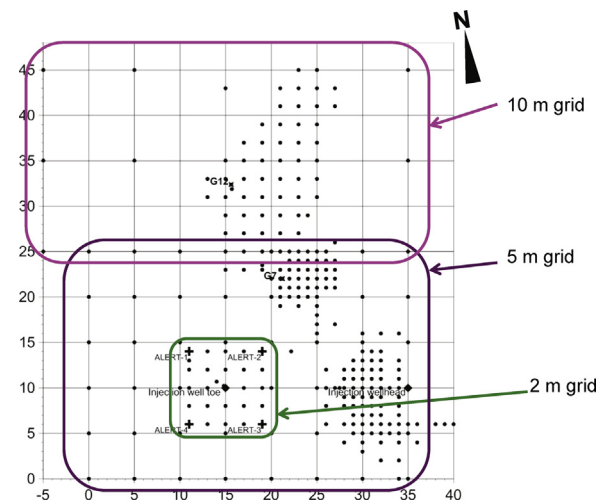
Fig. 3. Locations of survey sampling points on the local grid (in m). The small grid (green) surrounds the injection point, within the larger grid (purple) and its northward extension (pink). Other points provided detail in areas of surface leakage of CO_2. ALERT1 to 4 are four electrical resistivity tomography wells equipped with water sampling ports.

are described elsewhere (Gal et al., 2013). Geophysical monitoring included resistivity (downhole and tomography), ground penetrating radar and downhole gamma and electrical logging (described by Barrio et al., in press).

3.1. Deployment

A rectangular grid of soil gas and flux points with a 5 m spacing was set up by BGS in July 2011 with the injection point near its centre (Figs. 3 and 4). This extended 35 m E–W and 25 m N–S covering the flat part of the site, bounded by the track to the N, slope to the S, injection well head to the E and portacabin to the W. A more detailed 2 m grid was set up in the 8 × 8 m central area covered by geophysical monitoring (Fig. 3). These grids were used for baseline soil gas and flux readings in July and for measurements associated with the injection experiment in September. The area was extended for the experiment over a 40 × 20 m area to the north, with 10 m spacing, to cover possible updip migration of CO_2. Once leakage at
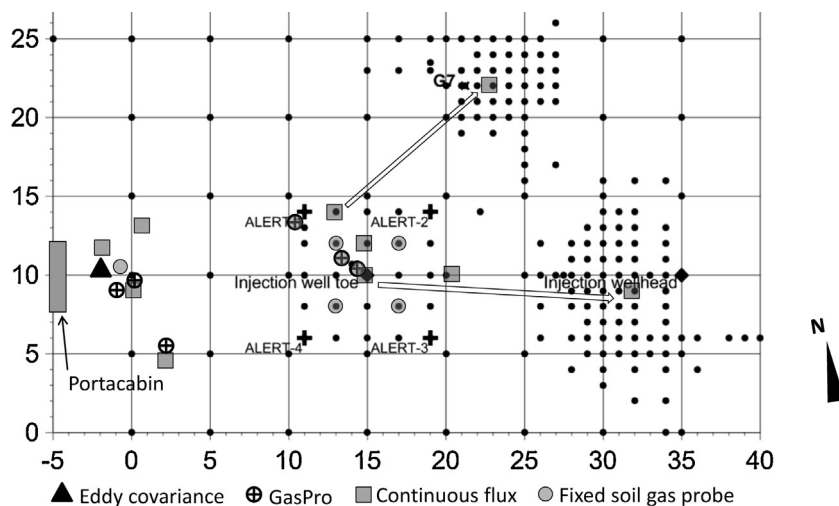
Fig. 4. Locations of BGS fixed monitoring equipment on the local grid (in m): baseline locations of GasPro gas monitoring station and continuous flux chambers are shown just east of the portacabin. Locations during the experiment are those in the central area (arrows indicate the positions that flux chambers were moved to once surface leakage was detected). Static laser measurements were made above the injection well toe and adjacent to the flux chamber near the injection well head.
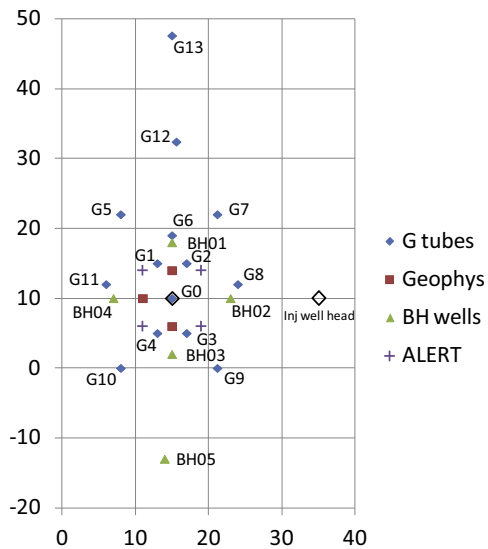
Fig. 5. Locations of BRGM monitoring on the local grid (in m). Soil gas was sampled at points G0–G13, continuous gas measurements made by 'Barasol' and 'Gasclam' near G6 and BH01 with isotope monitoring in BH01. Water sampling was done in ALERT and BH wells and other wells mostly outside this area to the north (not shown). Injection well toe was at G0.

surface was identified, more detailed patterns (with 1–2 m spacing) were measured to delineate it.

The EC system was set up 17 m to the west of the injection well toe, close to the portacabin (Fig. 4) and remained in this position until the end of the injection experiment. The continuous flux and soil gas equipment was initially placed near the EC tripod to avoid it being damaged during the drilling of the monitoring wells. It was then moved into final position at the start of the experiment on 5 September 2011 (Fig. 4).

Fixed soil gas probes were also placed adjacent to each of the buried continuous GasPro sensors in September to provide an independent assessment of their calibration and 4 probes were placed in a 4 × 4 m square with the injection well at its centre, whilst a final fixed probe was installed near the EC system, 15 m W of the injection point (Fig. 4). Repeated measurements were made at these points throughout the experiment.

Fourteen fixed gas probes were also sampled by BRGM on a daily basis (Fig. 5). CO_2 and C isotopes were measured continuously in

BH01, CO_2 was also measured in one adjacent shallow borehole and Rn in another (Fig. 5), as well as one to the north-west away from the injection area.

4. Results

4.1. Weather

Weather data were recorded from 25 July to 15 September 2011, but the rain gauge did not function correctly after the end of August. Atmospheric air temperature and barometric pressure readings were highest in late July and early August, with lower humidity. Conditions after 7 August were similar to those during the injection period. Barometric pressure varied from 1003 hPa at the start and end of the injection period to 985 hPa on the morning of 7 September and 980 hPa on the morning of 13 September. The highest pressure (1006 hPa) was recorded on the afternoon of the 10th. The low pressure was associated with heavy rain, from about 16:00 on 6 September and overnight into the 7th and during the day on 12 September and the evening of the 13th. This had some effect on near surface gas data, particularly affecting flux values for some hours immediately after the heavy rain, but given the very high permeability of the ground these effects were not long lasting. Free gas could nearly always be sampled at 50 cm depth even after rainfall.

Air temperatures varied between minima of 6 and 13 °C and maxima of 20–25 °C with the lowest diurnal range during the low pressure periods. Humidity levels varied from night time highs of up to 96% to daytime values as low as 40–50% (minimum 33%) during the finest weather. Wind speeds were generally low, mostly below 2.5 m s^{-1} but reached 3.9 m s^{-1} on 13 September i.e. light breezes on the Beaufort wind force scale. The strongest gust was only 5.5 m s^{-1} (gentle breeze in Beaufort terms).

4.2. Baseline measurements

Observations were made by BGS on the survey grids on 26–27 July 2011 and immediately before injection on 6 September. Continuous BGS baseline monitoring took place from the July dates until 5 September and was recommenced later that day after the instruments had been relocated to their experimental positions.

The soil CO_2 concentrations and surface CO_2 flux values were low for both sets of baseline observations (Figs. 6 and 7) although there were small differences. Mean and median CO_2 concentrations
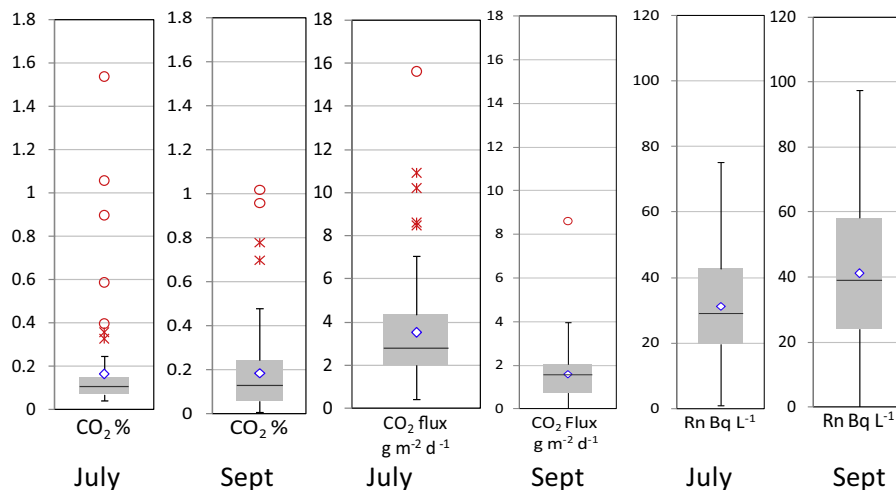
Fig. 6. Box and whisker plots of baseline soil gas CO_2, CO_2 flux and radon in July and immediately before injection in September 2011 (diamond shows mean value, asterisks are possible outliers, circles probable outliers).
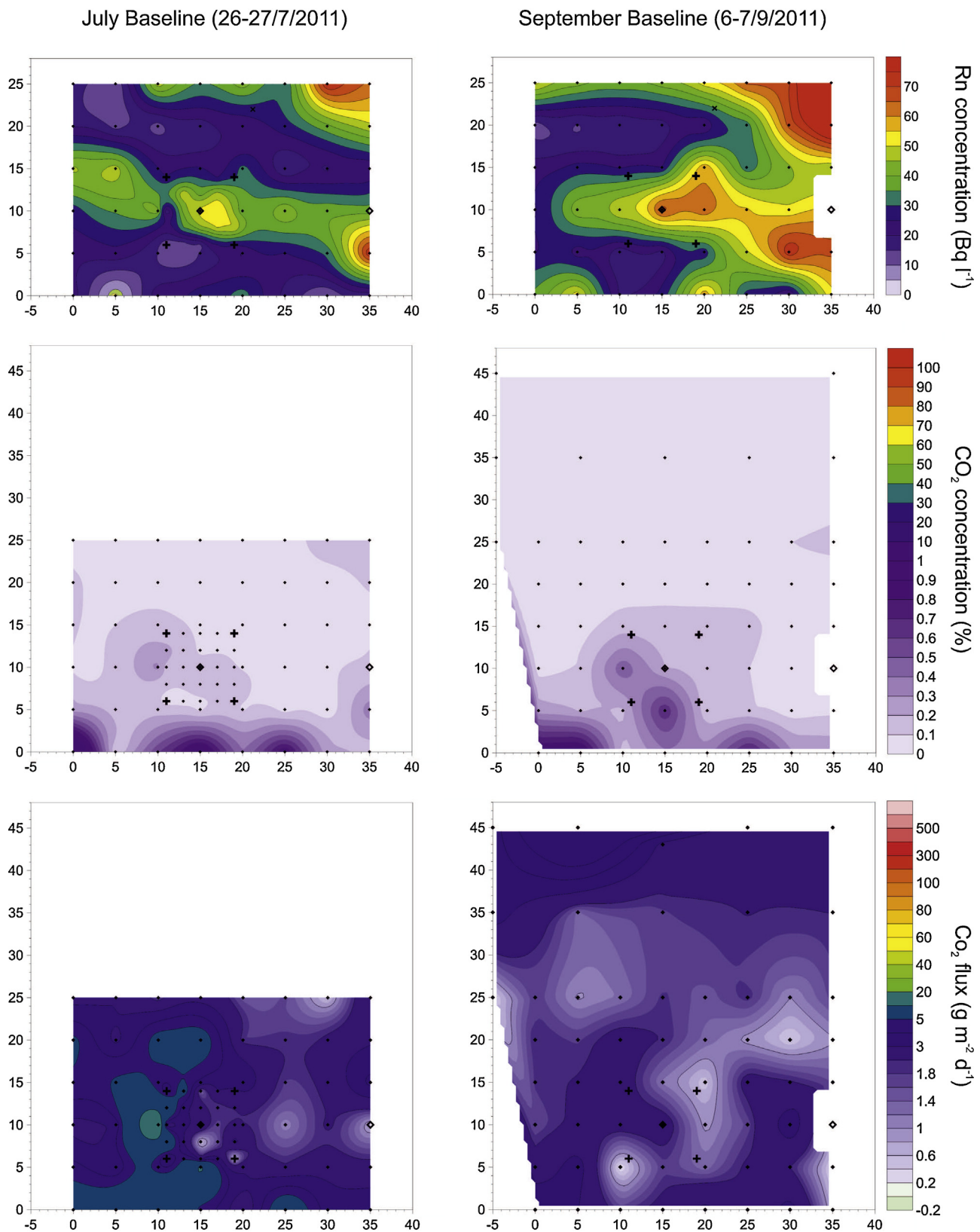
Fig. 7. Baseline survey data for soil gas and flux for July (left) and just prior to the start of injection in September (right) plotted on the local grid (in m). Diamonds show head and toe of injection well, crosses ALERT wells, points are sampling points.

were similar at less than 0.2%, but the spread of most values was slightly greater in September (3rd quartile of 0.25%, with 0.15% in July). Fluxes were significantly higher in July albeit still at low levels (maximum of 15.7 and median of $2.8 \, \text{g m}^{-2} \, \text{d}^{-1}$ compared with 8.6 and $1.6 \, \text{g m}^{-2} \, \text{d}^{-1}$ in September). Similarly low levels of both concentration and flux were obtained from a smaller number of measurements during a site appraisal in September 2010 (Bakk et al., 2012).
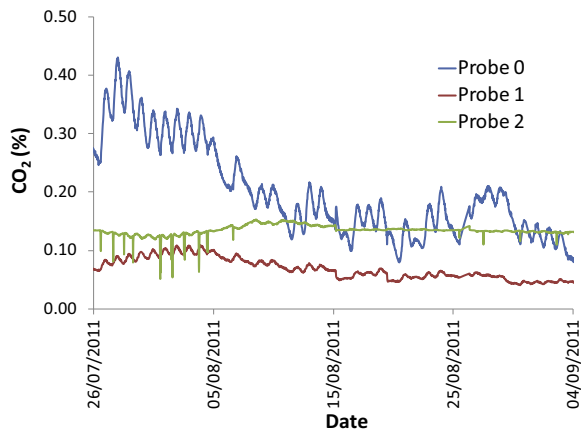
Fig. 8. Soil gas CO_2 data for the buried monitoring probes (at 50 cm depth) over the baseline monitoring period.

BRGM baseline data, consisting of 5 days of observations just prior to injection at the 14 fixed sampling tubes, also yielded a low mean CO_2 concentration of 0.12%. This is consistent with appraisal levels recorded across the whole Svelvik Ridge in 2010, including vegetated areas, which gave a mean of 0.37%.

Radon concentrations measured by BGS (Figs. 6 and 7) were moderately high and, like CO_2, showed an increase in mean levels and the range of values in September (mean and median of around 30 Bq L^{-1} in July and 40 Bq L^{-1} in September; range extending to almost 80 Bq L^{-1} in July and 100 Bq L^{-1} in September).

The highest flux value in July (nearly 16 g m^{-2} d^{-1}) was located 5 m west of the toe of the injection well, but this was not replicated in September (Fig. 7). The radon map in July showed a band of higher values almost coincident with the line of the injection well but extending westwards to the edge of the area surveyed (Fig. 7). This was flanked by lower levels to the north and south. Higher values were again apparent in the NE corner of the grid. The pattern was similar in September, with again the highest concentrations in the NE corner (Fig. 7).

4.2.1. Continuous measurements

The buried GasPro CO_2 monitoring sensors also recorded low CO_2 concentrations that were all below 0.45% (Fig. 8). Levels varied between the three probes over the 40 days of recording as did the extent of the diurnal variations, which were most prominent in probe 0 and most muted in probe 2, but did not normally exceed 0.1%. Longer term trends were also apparent and of slightly larger magnitude, with a general fall in CO_2 concentrations in all 3 probes over the last two thirds of the period.

The continuous monitoring with the GasClam gave CO_2 values below 0.1% both during the baseline and injection periods.

The four continuous monitoring flux chambers all showed a very clear diurnal pattern with values generally no higher than 4 g m^{-2} d^{-1} and a daily variation of 1–3 g m^{-2} d^{-1} over the baseline period, although recording stopped on 6 August when the solar panels were unable to provide sufficient charge to the battery powering the installation.

Baseline temperature and pressure conditions from the EC system exhibited a wide range of fluctuations over the month, with daytime temperature highs and nightly lows creating a sinusoidal diurnal pattern also seen in the weather station data. Large scale pressure oscillations represented weather systems moving across the site. For comparison of CO_2 concentration and flux data it was important to find a period in the baseline where atmospheric conditions were similar to those during injection, as temperature, pressure, wind speed and direction can have a major impact on

CO_2 release at the ground surface. The period 6th–15th August was selected as it was the same length as the experimental injection period and atmospheric variables, and the trends, were similar. Also this was a period when there were no other activities on site, as the drilling of the injection well was completed and work on the monitoring wells had not been started.

4.3. Injection experiment measurements

The 5 m grid was repeated on 8 September (following the start of injection at 10:00 on 7 September) with similar results to the baseline surveys (Fig. 9) until a point was measured 5 m W of the head of the injection well, at 14:51 local time (UTC + 2), with a CO_2 concentration at 50 cm depth of 86%. Investigations around this point showed values to the E of almost 100%. The area of venting was then covered by a 1 m grid of CO_2 concentration and flux readings, showing a near circular zone of high CO_2 concentrations approximately 8 m across, centred about 4 m WSW of the head of the injection well, and a smaller (about 3 m diameter) patch of high CO_2 flux, with a maximum value of 1886 g m^{-2} d^{-1}, centred only 1 m W of the head of the injection well (Fig. 9). Two lobes of higher flux extended out from this some 4 m to the SW and 5 m to the WNW.

The initial area of gas venting was re-examined the following day (9 September) with a 2 m grid (Fig. 9). The area of high CO_2 appeared to have expanded slightly, perhaps spreading by up to 1 m. The area of higher fluxes seemed to match more closely to that of the CO_2 concentrations but with a clearer lateral expansion of some 2 m to the SW.

On 10 September the whole 5 m grid was repeated, showing the continued existence of the CO_2 vent just W of the head of the injection well and suggesting a further lateral spreading of higher values (Fig. 9). Also a higher CO_2 concentration was discovered at about 15:00 (UTC + 2) in one of the BRGM fixed soil gas sampling points (G7), located about 13.4 m NE of the injection point (6 m E and 12 m N). A series of 1 m spaced observations were made to delineate this second area of surface leakage (Fig. 9). The 5 m grid points to the NE and SE of this feature did not detect any CO_2 just over 2 h before the discovery but concentrations had risen slightly (from 0.0 to 0.8 and 0.2% respectively) when the points were re-measured some 5–6 h later. Concentrations of CO_2 reached a maximum of 97% at the centre of this second vent and the flux readings showed a similar pattern of values ranging up to 922 g m^{-2} d^{-1}.

Surveys on 11 September looked at the continued development of the initial vent near the injection well head and whether the second vent was linked to it at the surface (Fig. 9). Flux measurements showed that the flow of CO_2 was impeded significantly by the heavy rain that had fallen overnight and created near saturated ground conditions. The soil gas measurements confirmed the slow spreading of higher values suggested by limited data the previous day and indicated clearly that there was no near surface linkage between the 2 vents.

A third area of CO_2 leakage was discovered on 12 September at about 10:00 local time (Fig. 10) when higher CO_2 was seen by BRGM in the fixed gas probe G12, located 22 m N of the injection point. This was investigated with a 2 m grid and additional measurements were made to track the continued development of the other 2 vents.

This new area was more elongated than the others, being some 14 m N-S and 8–10 m E-W, based on elevated gas concentrations, and linked to the second vent. There were 2 new centres of higher flux, linked to the earlier vent. The stronger, more northerly, of these was 4 m N of the highest CO_2 concentrations, but the concentration plot is affected by a lower value in this area, which is likely to be the result of atmospheric dilution because it was only possible to insert the sampling probe to a depth of 30 cm. Maximum fluxes were over 1200 g m^{-2} d^{-1} at the most northerly point but only 390 and 230 g m^{-2} d^{-1} at the linked centres further S. The area
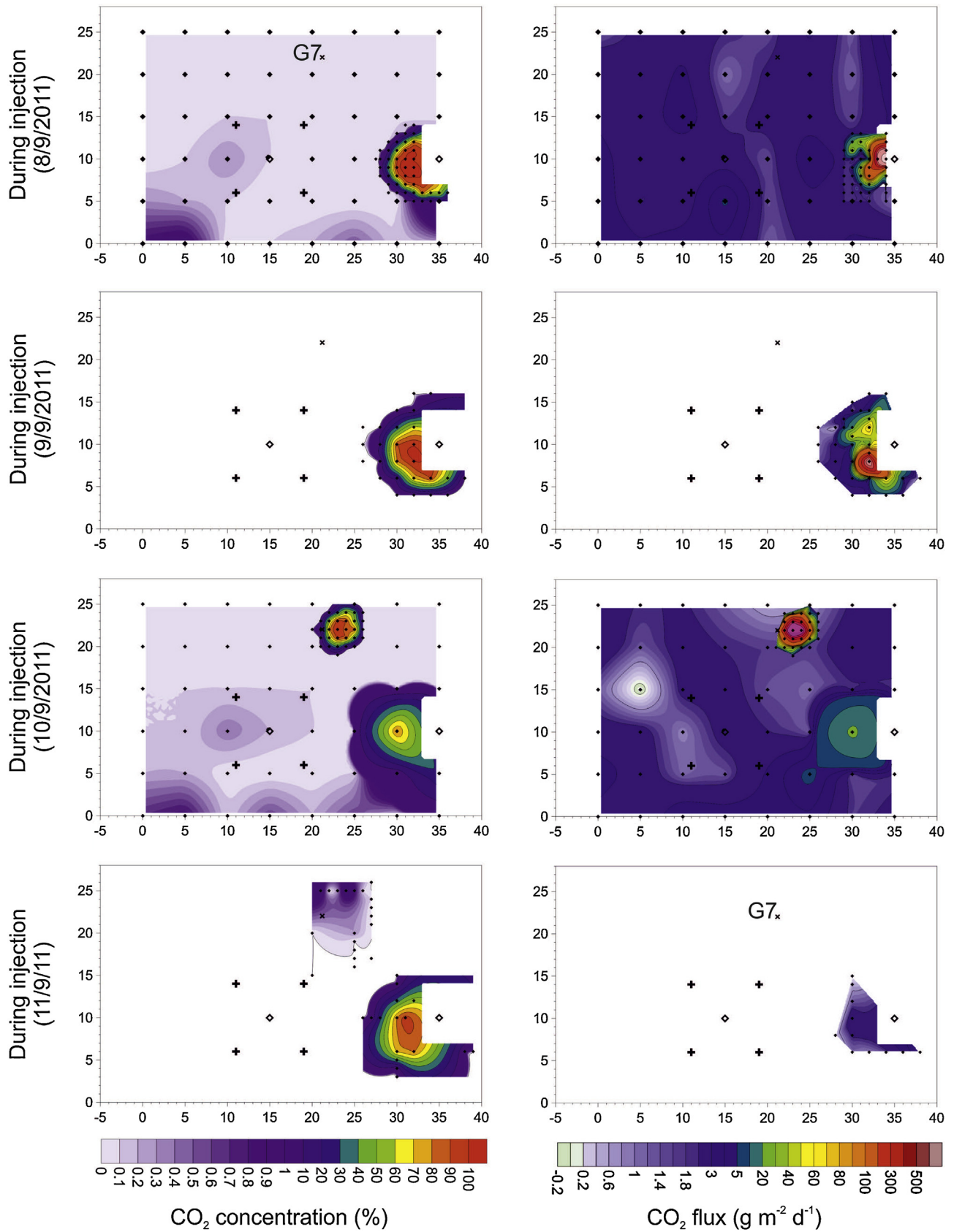
Fig. 9. Soil gas and flux data for 8–11 September showing gas escape near the head of the injection well and near G7. Diamonds show head and toe of injection well, crosses ALERT wells, points are sampling points.
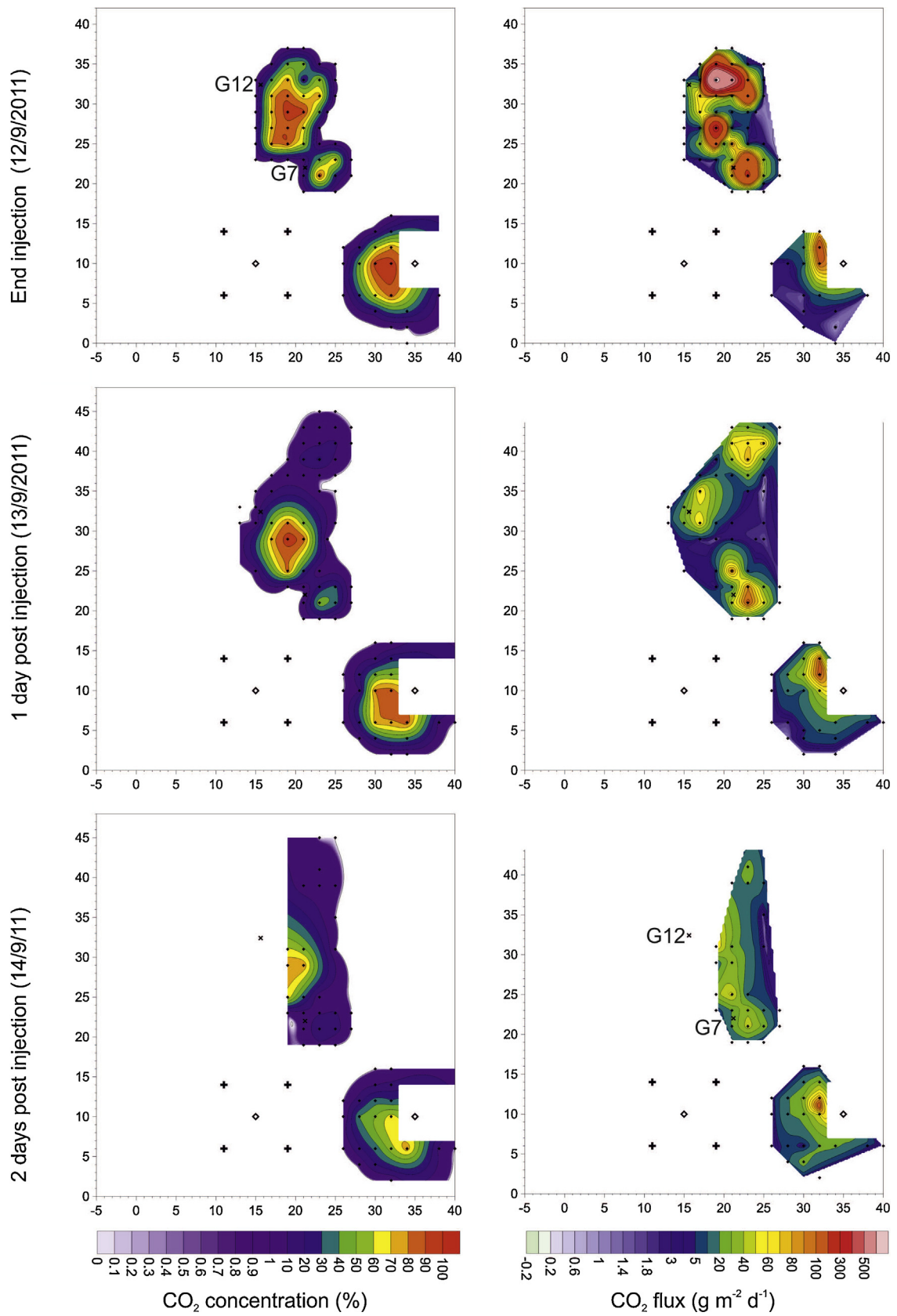
Fig. 10. Soil gas flux surveys 12–14 September showing 3 areas of gas escape including the new vent near G12. Diamonds show head and toe of injection well, crosses ALERT wells, points are sampling points.
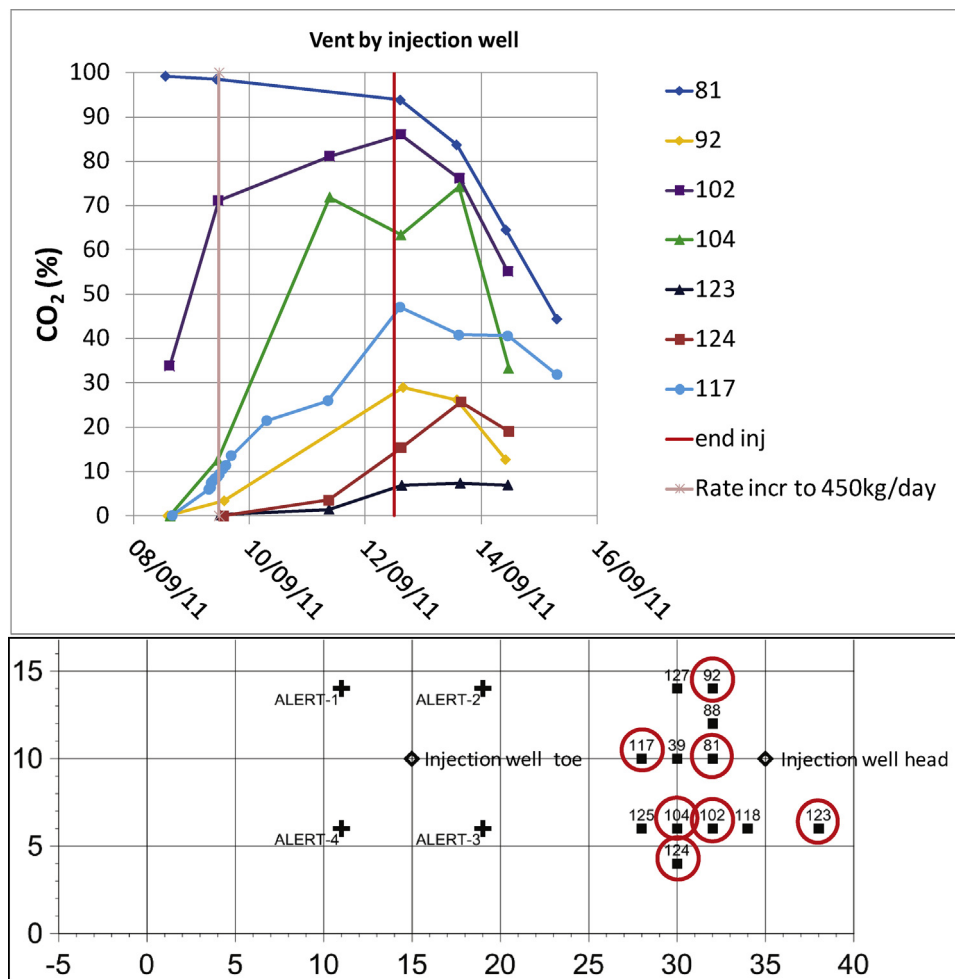
Fig. 11. CO_2 content of soil gas at 50 cm depth at selected individual locations through time, for the vent by the injection well: locations shown on the bottom map.

between the injection well and the northerly vents was tested on 11 September but no evidence for any surface leakage found. This confirmed previous observations of the 5 m grid on 10 September and measurements made on a few additional points on the previous day (not plotted).

The 3 vents show a strong NW-SE alignment, particularly in the CO_2 concentration data, with a more N-S trend apparent in flux and in the elongation of the northernmost vent. Measurements were made along this alignment to the SE of the injection well head but showed no indications of surface leakage.

Measurements were made of the pre-existing vents after injection ceased at 14:00 (UTC + 2) on 12 September. There was still evidence of a slight continued expansion of the outer edge of the injection well head vent and a small southward shift in the vent near G7.

On the following day the 2 most northerly points measured the previous day on the northernmost vent showed a slight increase in CO_2 concentration (1.5–2.2% and 3.1–4.8%) and a further area of higher values (up to 24%) was delineated to the NNE (Fig. 10). This could have been present, but unobserved, on the 12th. The core of the northern vent was smaller, with a reduced area with concentrations above 60%. The linked vent to the SE (near G7) showed a more obvious reduction in concentrations at its centre, with the highest value dropping from 89 to 48%. A similar fall was also apparent for the vent by the injection well. Flux rates showed a more marked fall, especially at the northerly vents, but they were affected once more by heavy overnight rainfall.

On 14 September all the gas leakage areas showed a clear continued fall in concentrations (Fig. 10). The reduction in flux was less pronounced because the drying ground conditions allowed the CO_2 to escape more freely. The few final measurements on 15 September showed a further fall in gas concentrations and fluxes for the vent near G12.

The changes in gas concentration at individual locations over time were broadly in accordance with the spatial variations. Values in general increased during injection and then fell away almost immediately once it had ceased, as illustrated for the vent near the injection wellhead (Fig. 11). Thus, in most places, a steady state had not been reached that reflected the constant injection rate over the final 3 days of injection. The pattern was different at individual points because the CO_2 vents spread over time and this continued post-injection. A further complication is that the probes may not have been inserted each time at precisely the same point, or exactly the same depth, so that small scale spatial (mostly on a scale of a few centimetres) and depth-related variability may also be present. Probes were left in place at a few locations (e.g. at point 117) to avoid these effects, but there were not sufficient spare probes to allow this at a large number of points.

4.3.1. Atmospheric and continuous measurements

When injection commenced CO_2 was observed escaping directly from the wellhead injection system into the atmosphere. The gas emitted was measured with a flow meter and could therefore be subtracted to obtain the total amount of subsurface injected gas.
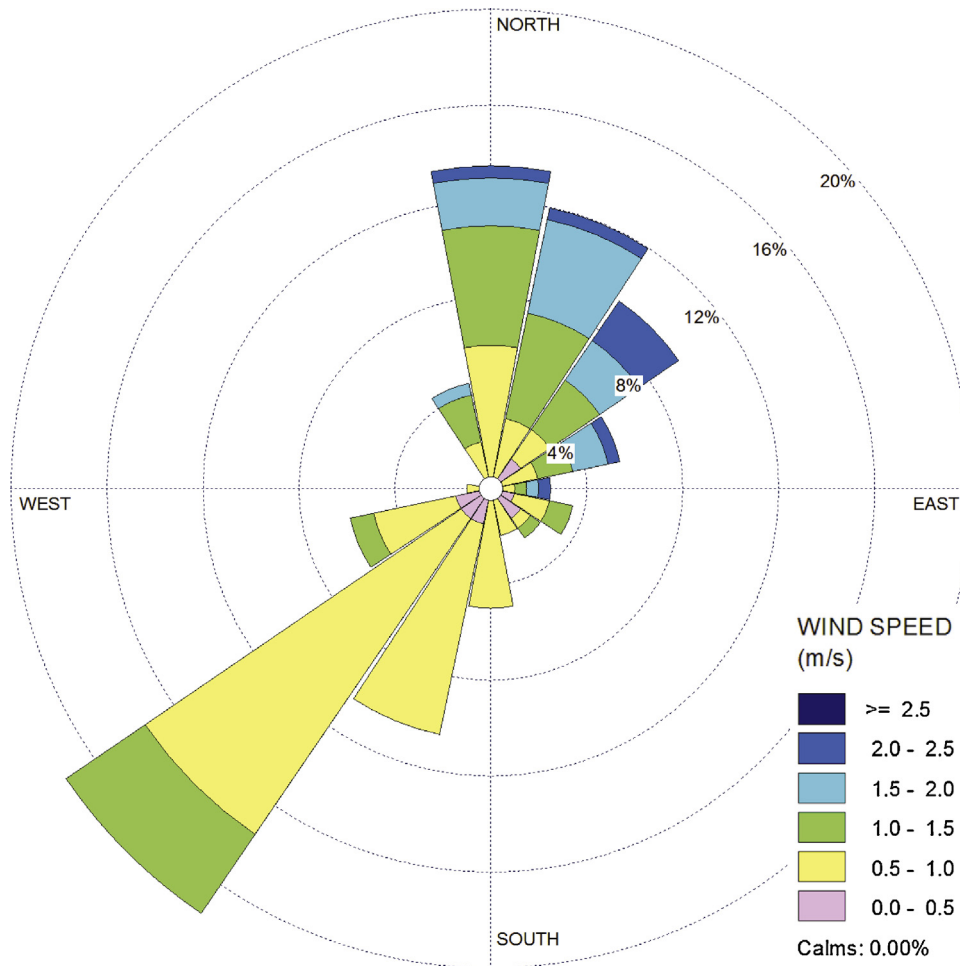
Fig. 12. Wind rose for the September monitoring period.

However, this above ground source had a potential impact on atmospheric gas measurements (i.e. the open path laser and eddy covariance methods) making the recognition of seepage from the subsurface more difficult with these techniques. They were also potentially affected by vehicle movements and the need to provide power from generators, although efforts were made to keep vehicles and generators as far away from the experimental area as possible.

4.3.1.1. Eddy covariance. Wind direction and speed play an important role in transporting gases released from the ground surface to the point measurement location of the EC system. The low wind speeds experienced during the measurement period reduced the size of the CO_2 source footprint calculated for the EC system, potentially enhancing its ability to detect CO_2 leakage. However, during the injection phase of the experiment, the wind direction was not generally conducive to observing a response to the surface CO_2 leakage described above (Fig. 12). Air flows during the injection period were low with slightly higher wind speeds from the N to NE interrupting calmer periods of flow from the SW. Only rarely (approximately 20% of the time in September) did the wind come from the E to NE from the areas of surface CO_2 leakage.

A diurnal pattern in CO_2 concentration and flux can be seen in the data (Fig. 13). The ranges of CO_2 concentrations and fluxes were comparable for both the baseline and injection periods, with no significantly higher values in September, at least for the 30 min averages. CO_2 flux increases during the injection period suggest that a greater component of measured CO_2 is sourced from the

terrain surface. This contrasts slightly with the baseline data which suggest that the terrain overall was acting as a CO_2 sink. However, this shift to positive flux was only slight and the trend could have been caused by influences external to the experiment.

Flux footprints were calculated as an average over the selected baseline and injection periods (Fig. 14). Both periods show a similar distribution where the most likely CO_2 source areas are within the immediate vicinity of the instrument, and likelihood tails off towards the predominant wind directions (i.e. to the SW and NNE). Because the vents occurred at greater than anticipated distance from the EC, and the wind speeds were low and variable in direction, the chance of their detection by the EC was reduced. As the flux footprints are similar in spatial distribution, and that for the injection period shows no bias towards a particular direction in comparison to the baseline data, it is unlikely that the injection experiment had a significant impact on atmospheric CO_2 at the point of EC measurement.

EC data were also averaged for both a pre-injection and during injection period (6 and 9 September respectively) at 1 Hz intervals (Fig. 15) to see if leakage could be detected in much shorter time period data. This showed similar base levels for both days but generally more noisy data prior to injection, particularly after about 14:00 h UTC (16:00 local time). On the 6th the wind was almost entirely from a westerly quadrant (NW-SW) suggesting possibly higher CO_2 from a generator located on that side of the site. In contrast, there was an easterly air flow on the 9th, in the first half of the day; the greater variability in the CO_2 concentrations over that period, compared with the 6th (except between 0400 and 0500 on
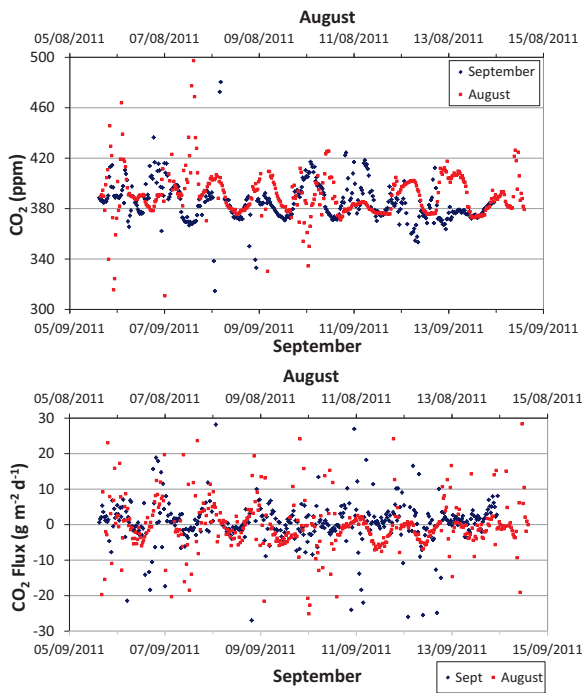
Fig. 13. Comparison of CO_2 concentration (top) and derived CO_2 fluxes (bottom) over the selected baseline (August) and injection (September) periods. The negative gradients of CO_2 over the periods are linked to the observed increases in temperature.

the 6th) may reflect the leakage of CO_2 associated with the experiment. However, this could be from the CO_2 escaping directly to the atmosphere at the well head or the seepage through the ground from the injected CO_2.

4.3.1.2. Open path laser. The laser system was used to make static measurements at the ground surface just above the injection point for variable periods during the first 5 days of the experiment, from 5 September to 9 September (Fig. 16). No data were recorded on the morning of 6 September owing to problems with the GPS signal.

There was a marked variation in CO_2 concentrations during this period, with values ranging from 330 to over 800 ppm. The relatively small amount of pre-injection data (for 5 and 6 September) falls in the lower part of the overall range (340–420 ppm) but overlaps with results during injection (7–10 September) for the same time of day. Previous experience suggests that short-term variations (over a few seconds) are more indicative of CO_2 leakage than changes over minutes or hours (Jones et al., 2009) and it does appear that short term fluctuations are more marked during injection, where spikes that exceed 100 ppm in amplitude can be seen (Fig. 16).

However, interpretation of the data in terms of seepage from the injected CO_2 through the ground, is made more difficult by the direct escape of CO_2 to the atmosphere at the injection well head, just over 20 m from the measurement point. In the light wind conditions this may have caused a general build up of CO_2 concentrations, with the gentle breezes carrying CO_2-enriched air through the laser beam. The leak was partially contained within the concrete ring that protected the injection well head, which gave rise to CO_2 concentrations there that reached low percentage levels. Gaps between the concrete structure and the ground surface allowed some gas to escape at near ground level into the surrounding area; the top of the ring was capped by a concrete lid, but this probably did not form a perfect gas tight seal. The above ground escape of CO_2 makes
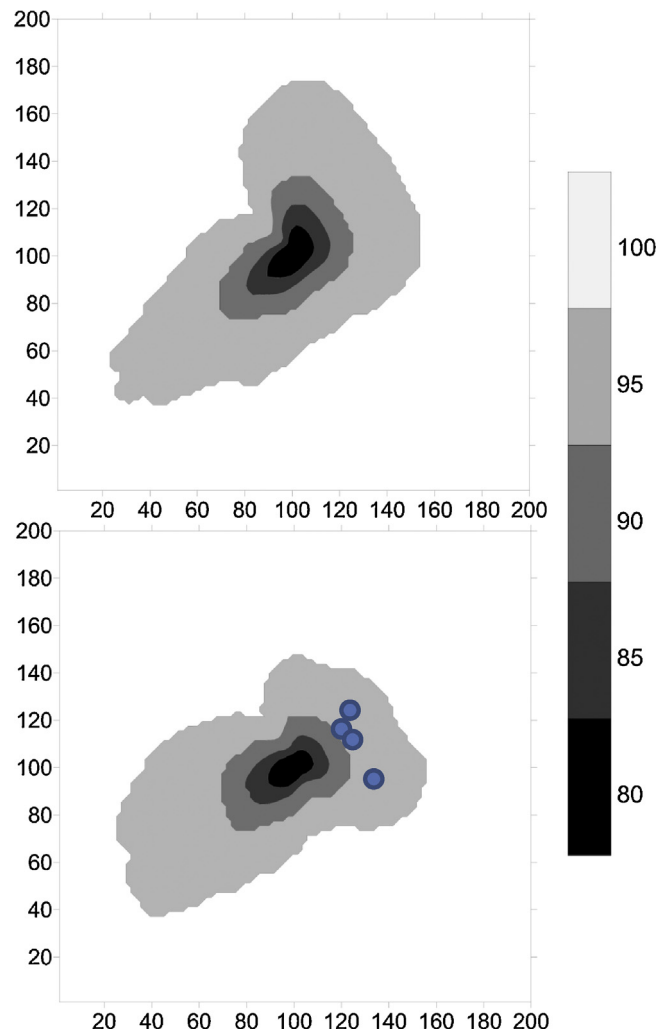
Fig. 14. North orientated plan view of CO_2 flux footprint as a percentage over the selected measurement times (baseline – top and injection period – below). The greyscale represents the percentage chance of CO_2 being sourced from that area. The EC was located in the centre of the plot. Vent locations shown approximately as blue circles. *X* and *Y* scales are in metres.
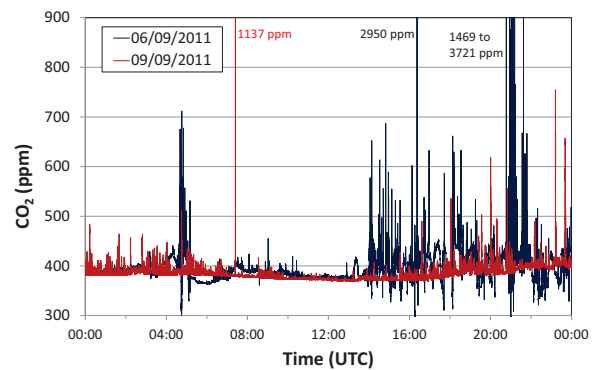
Fig. 15. 1 Hz averaged EC CO_2 concentrations for 24 h periods prior to injection (6 September) and during injection (9 September). Values are shown for off scale points.

it very difficult to separate out any response caused by CO_2 seeping through the ground from the injection.

It would be expected that the well head leakage would give a less pronounced response in CO_2 concentrations for the eddy covariance system, as this was roughly twice the distance away and
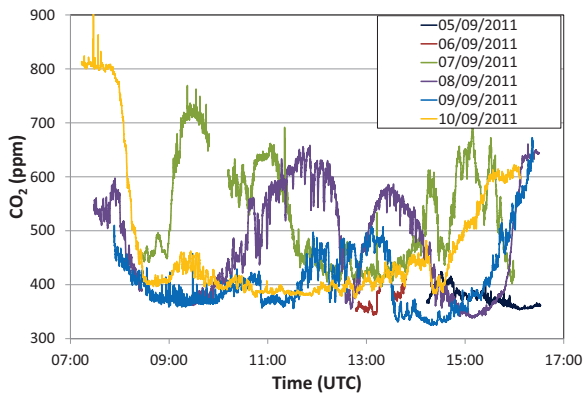
Fig. 16. Static measurements with the open path laser system in the air immediately above the injection point, probably affected by above ground leakage from the wellhead during CO_2 injection.

Fig. 17. Mobile laser measurement of CO_2 (ppm) from the main experimental area overlain on soil gas data for 9 September to show the position of CO_2 vents at the time. Values outside this area were all below 350 ppm.
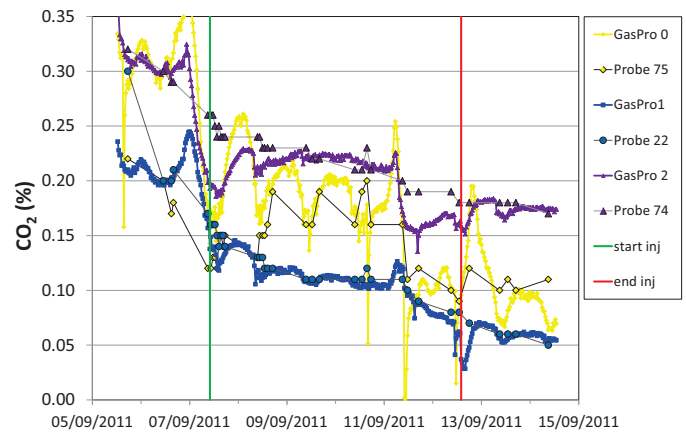
Fig. 18. Comparison of continuous soil gas monitoring data from the three buried GasPro sensors (0, 1 and 2) and the fixed soil gas probe measurements. GasPro 1: close to the well toe, next to Probe 22. GasPro 2: 1.2 m from the well toe, next to Probe 74 and GasPro 0: 5.0 m from the well toe, next to Probe 75.

atmosphere at the wellhead is the likelier source of the higher values. There was also no apparent signal from the more northerly vent, but this was not discovered until the following day and may not have been developed at this time. The pattern of highest values just N of the injection well head and a broad band of slightly higher values just N of this may indicate a northward drift of CO_2 from the well head; the average recorded wind speeds at this time were less than $0.3\,ms^{-1}$ and variable in direction. Values outside the experimental area were uniformly low (Fig. 17).

4.3.1.3. Continuous soil gas monitoring. The three CO_2 GasPro units buried in the central area (above the well toe, but far from the mapped leakage areas discussed above) continued to show the overall declining trend that was apparent in the period of more than 3 weeks prior to injection, with good agreement between the GasPro data and the manual samples collected from the fixed probes. Some diurnal variations are superimposed on this general trend, most notably in probe 0 located furthest from the injection point (Figs. 8 and 18). The diurnal changes of up to 0.1% were as large as any other variations over the injection period. Therefore any effects that might be due to surface leakage of CO_2 were hidden within the normal background variability. The GasClam similarly showed no indication of leakage, with values remaining below 0.1% throughout the monitored period.

4.3.1.4. Continuous accumulation chamber flux monitoring. The continuous flux monitoring above the injection point continued to show diurnal patterns comparable, even if of lower amplitude, to those seen in the July–August period for all four chambers when deployed in the central area above the injection point (Fig. 19). Flux rates there did not exceed $2\,g\,m^{-2}\,d^{-1}$ and were suppressed by the periods of heavy rainfall. When Chamber 1 was relocated to the vent nearest the injection well head, flux rates continued to rise from around $70\,g\,m^{-2}\,d^{-1}$ to over $450\,g\,m^{-2}\,d^{-1}$. This was sited a little way from the centre of the vent and thus does not represent the maximum flux rates. On the other hand the fluxes on the second vent near G7, which were recorded close to the vent centre, climbed initially from $436\,g\,m^{-2}\,d^{-1}$ to a maximum of $803\,g\,m^{-2}\,d^{-1}$ then varied between 560 and $800\,g\,m^{-2}\,d^{-1}$. The flux rates fell steeply at both locations when injection was stopped, reaching similar minima between $20–30\,g\,m^{-2}\,d^{-1}$. The reduction in fluxes just after injection stopped was exaggerated by heavy rainfall later the same day, which impeded surface flow. Fluxes then rose as the ground dried out before decreasing once again. Both flux units deployed on the vents had reached $34–35\,g\,m^{-2}\,d^{-1}$ at the end of the

at a greater height. Data (1 Hz averages) from the EC were compared with the static laser results from one pre-injection period (6 September) and one during injection period (9 September). The EC data for 6 September compare quite closely to the more limited laser results (Figs. 15 and 16), but the complete EC profile showed a change after about 14:00 (UTC) when the CO_2 concentrations became much more variable. This suggests a source of CO_2 relatively close to the EC. In contrast the post-injection example presents a flatter profile with only minor spikes, which are more pronounced at the start and end of the plotted period. This does indeed show a much reduced variability compared with the laser results.

Mobile laser measurements were made on 11 September, both in the experimental area and, for comparison, further a field (Fig. 17). The highest values were just north of the injection well head. Again it is difficult to know if these result from the above ground escape of CO_2 or the seepage of CO_2 through the ground. The impact of the CO_2 seepage on atmospheric levels was very probably subdued by the wet ground conditions following heavy overnight rain immediately prior to these measurements. This may explain why the vent near G7 did not appear to produce a response in the mobile laser data and suggests the direct escape of CO_2 to

Fig. 19. Continuous flux monitoring data. Data for the chambers moved onto the vents (blue, green lines) are plotted on the left axis. Earlier data for these chambers are not included for clarity, as they are similar to those for Chambers 2 and 4.

measurements; clearly injected CO_2 was still escaping at this stage as both chambers above the injection point were only recording $0.5\,g\,m^{-2}\,d^{-1}$.

4.4. Carbon and oxygen isotopes

Six CO_2 samples measured for their $\delta^{13}C$ during the 2010 appraisal visit varied between −19.7‰ and −24.6‰. The 2 samples analysed in the laboratory from the 2011 baseline yielded $\delta^{13}C$ values of −16.0 and −24.4‰ compared with local atmospheric CO_2 at −11.9‰ and the injected CO_2 at −30.4‰.

The CO_2 concentrations, $\delta^{13}C$ and $\delta^{18}O$ of the injected gas and the local atmosphere, measured in the field, are reported in Table 1. The atmospheric background CO_2 concentration was at an expected level, while the corresponding $\delta^{13}C$ was slightly depleted in ^{13}C compared with the baseline measurement probably indicating the influence of vegetation in the surroundings of the site. $\delta^{18}O$ of CO_2 was consistent with values expected at these latitudes (Farquhar et al., 1993). $\delta^{13}C$ and $\delta^{18}O$ of the CO_2 from the injection tank were typical of industrially synthesised CO_2 (Deines, 1980). These two potential end-members exhibit significantly distinctive carbon and oxygen isotope compositions to allow them to be distinguished.

The continuous monitoring at 1 Hz frequency throughout the experimental period at BH01 (at 50 cm depth in this 2 m deep borehole) is reported as daily averages and standard deviations, both for CO_2 concentrations and corresponding $\delta^{13}C$ and $\delta^{18}O$ in Fig. 20. The CO_2 concentrations do not show significant variations over this period. The small variations seen are well within the diurnal atmospheric range observed with other methods. However $\delta^{13}C$ values show a large range of values varying between −4.6 and −27.1‰, which can be explained by a binary mixing between atmospheric and injected CO_2. The response appears to have been fairly rapid as the average data from 8 September already displayed a decrease in ^{13}C which can be linked to the injection of CO_2. Equilibrium seems also to have been rapidly reached as $\delta^{13}C$ was at a constant level from 3 days after injection started (10 September) until 14

September. There was therefore a delay after injection stopped on 12 September, until the carbon isotope composition returned to almost atmospheric values by the 15th (8 days after the start of injection).

Oxygen isotope compositions behaved in the opposite way to carbon with enrichment in ^{18}O during injection. This cannot be explained by a simple mixing between atmospheric injected CO_2 as $\delta^{18}O$ in BH01 was always higher than for these two end-members. When CO_2 and H_2O are in contact a thermodynamic equilibrium is reached between the oxygen isotopes of the CO_2 and the water. This leads to a shift in the $\delta^{18}O$ of the water without affecting its δD (Hofmann et al., 2012). At low temperatures the water is depleted in ^{18}O (i.e. its $\delta^{18}O$ decreases) whilst the CO_2 is enriched in $\delta^{18}O$. Results (Fig. 20) confirm that isotope interaction occurred between water and CO_2, increasing the $\delta^{18}O$ of the residual CO_2 measured in BH01. As for the carbon isotopes, the response was fairly rapid (apparent on 8 September) but equilibrium seems to have taken longer; $\delta^{18}O$ values were still increasing even after injection ended and reached a maximum on 14 September. This maximum could either indicate isotopic equilibrium or the end of CO_2 supply. Our data cannot distinguish between these two options. The recovery to baseline levels was slower and they had not been reached by 18 September.

Fig. 21 reports the coupled $\delta^{13}C$–$\delta^{18}O$ variations of CO_2 in BH01 during the experiment. Prior to CO_2 injection both isotope compositions were consistent with the local atmospheric CO_2 end-member. When injection started a rapid decrease in $\delta^{13}C$, coupled to an increase in $\delta^{18}O$ was observed. Isotope equilibrium was then reached for carbon while $\delta^{18}O$ was still increasing. When CO_2 injection ended, both $\delta^{13}C$ and $\delta^{18}O$ rapidly returned towards initial values although recovery was not totally completed by the end of monitoring on 18 September (Table 2).

5. Discussion

Baseline data for both the initial site assessment in 2010, and for the July to early September period preceding the experiment, indicate low levels of soil gas CO_2 and low CO_2 flux rates making a leakage signal from the experiment relatively easy to detect by such measurements.

Surface leakage was clearly seen by an obvious rise in both the CO_2 concentrations in the soil gas and flux in and around a number of seepage areas. This is confirmed by the relationship of CO_2 to both O_2 and 'balance' (where balance is the percentage remaining after the gases detected are subtracted from 100%. This would be expected to comprise largely N_2 with minor Ar and other trace gases). In biological reactions O_2 is consumed at the same rate as CO_2 production and therefore reaches zero for a CO_2 content of around 21% (Beaubien et al., 2013; Romanak et al., 2012). Nitrogen is unaffected and therefore does not change with increasing CO_2. On the other hand, when injected CO_2 escapes there is a dilution of both O_2 and N_2 and hence these trend towards zero for 100% CO_2. Such a dilution effect is clearly visible in the data from Svelvik (Fig. 22).

Outside the seepage areas, including in the central area above the injection point, there was no sign of leakage from concentrations or fluxes either in intermittent surveys or more continuous measurements. However, the C and O isotope data, albeit measured at 50 cm depth, suggest that low level leakage was occurring in this area, although this did not give rise to a detectable change in the overall level of CO_2. Perhaps because the overall background levels of CO_2 were falling over the experimental period (as indicated by all the other measurements in the central monitoring area). In this case the isotope measurements appeared to be extremely sensitive to leakage, even when the amounts involved were very small.

Table 1
CO_2 concentrations and isotope compositions for atmospheric background and injected gas.

End-member	CO_2 concentration (ppm)	$\delta^{13}C$ CO_2 (‰ vs PDB)	$\delta^{18}O$ CO_2 (‰ vs SMOW)
Atmospheric background	384	−13.7 ± 0.1	28.6 ± 0.2
Injection tank	10^6	−30.4 ± 0.1	12.9 ± 0.1
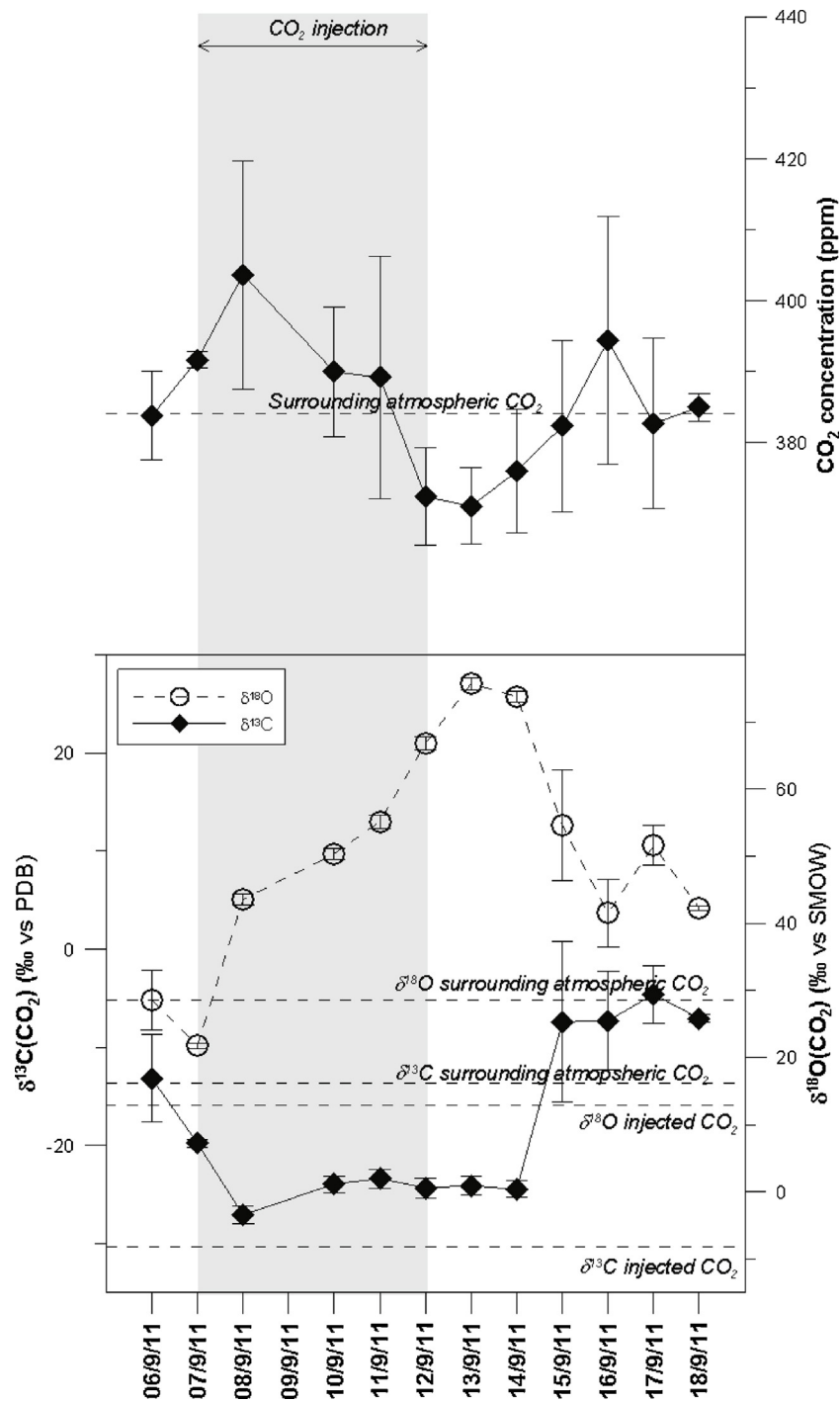
Fig. 20. Variations in CO_2 concentration (top) and carbon and oxygen isotope ratios (bottom) measured in BH01 during the experiment.

This is because the isotopic signature of the injected CO_2 was sufficiently different from that of atmospheric CO_2, albeit a likely low level biological CO_2 contribution, measured in the range −16 to −24.4‰, has been ignored. Such differences between the isotopic signature of the injected CO_2, and ambient soil or atmospheric CO_2, has been used to advantage in other injection experiments, such as those conducted for the RISCS project (Moni and Rasse, 2013) and at the ZERT site in Montana (Fessenden et al., 2010; Krevor et al., 2010; McAlexander et al., 2011), where low levels of leakage were discernible by C isotope studies. In real CO_2 storage sites leakage detection using C isotopes is not necessarily possible even for relatively high concentrations of CO_2 depending on the source, and hence isotopic signature, of the injected CO_2. For example, at the Weyburn site in Canada there is overlap between the isotopic signatures of the injected and reservoir CO_2 and the near-surface biological component (Beaubien et al., 2013; Risk et al., 2013; Trium, 2011). Thus stable C isotopes are not a clear indicator of leakage and other approaches, including gas ratios (O_2 and N_2 to CO_2), radiocarbon and noble gas isotopes, have proved to be much better at discriminating near surface biogenic CO_2 from leakage of CO_2 from depth (Beaubien et al., 2013; Gilfillan and Haszeldine, 2011; Romanak et al., 2013; Trium, 2011).
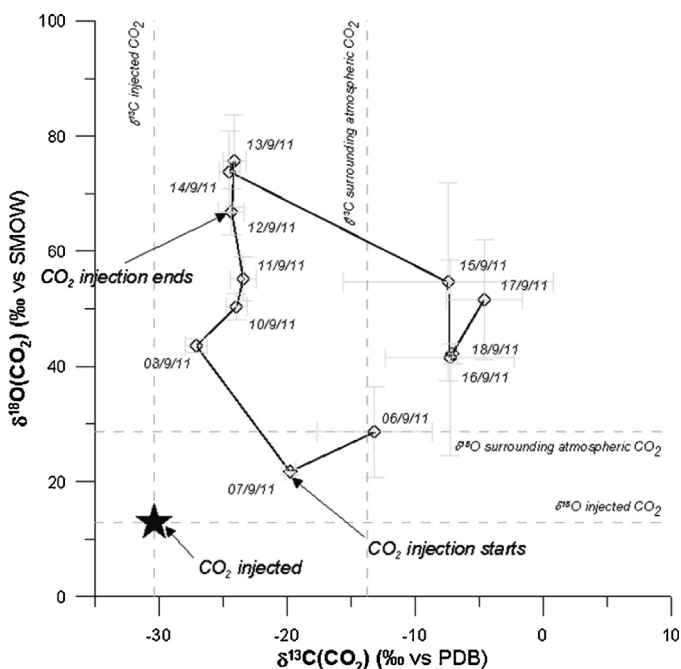
Fig. 21. Dual isotope ($\delta^{13}C$ & $\delta^{18}O$) monitoring of the CO_2 above the water table during the experiment.
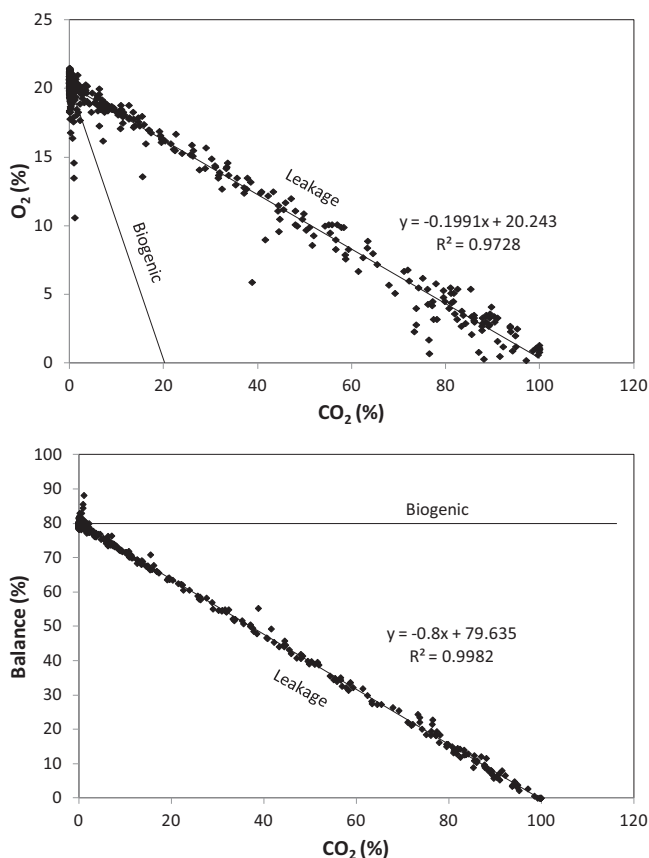
Fig. 22. Relationship between CO_2 and O_2 and balance (mostly equivalent to N_2) in soil gas data from the shallow injection experiment at Svelvik.

Alignment of the vents could indicate more permeable pathways broadly updip (N-S) and oblique to dip. These may be indicated in a general way by the pattern of Rn concentrations, which broadly align with the general E-W strike of the sediments (Fig. 7), although these may result from compositional changes

(variations in ^{238}U and other Rn parents) as well as permeability effects.

The smallest vent near G7 would have been difficult to detect with the 5 m soil gas and flux grid because it fell neatly within a square bounded by 4 of the grid points. It was fortuitous that the fixed sampling tube at G7 fell within this grid square and on the edge of the area of seepage, enabling this vent to be identified and delineated. It is possible that other small areas of surface leakage went undetected because they fell between the grid points or because attention was diverted to monitoring the known areas of seepage and hence the full grid was not repeated regularly in the latter stages of injection. However, any missed areas could not have been large as they were not detected by the regularly monitored fixed points or evident in the EC data.

Heavy rain had a significant effect on the soil gas concentrations and reduced the flux of CO_2 for several hours, even in such a high permeability and free-draining substrate. Rainfall has been inferred to act as a physical barrier to flow and, in larger amounts, cause dissolution and displacement of gases (Hinkle, 1994). Flux then increased once free pathways to the surface were re-established. There was not a consistent pattern of flux from the continuous flux monitoring of the first two CO_2 vents detected. The initial occurrence, near the injection well head, showed a general pattern of rising flux consistent with the ramping up of the injection rate over time, but continued to rise even when the injection rate was constant for the last 3 days of injection. In contrast the second vent near G7, after an initial increase, gave more variable fluxes suggesting pulses of CO_2 release. This might perhaps be related to the development of the further venting area to the north, which was first detected during a dip in the flux rate at the G7 vent and which caused a diversion of flow from the earlier vent.

The maximum flux observed approached 2000 g m^{-2} d^{-1}. This is similar to flux rates observed at natural CO_2 vents (e.g. Beaubien et al., 2008; Krüger et al., 2011; Lewicki et al., 2007; Lombardi et al., 2008; Pettinelli et al., 2010). However, the areas of highest flux were spatially limited to a few m^2. It is difficult from the measurements made to arrive at an accurate estimate of the total leakage of CO_2 from the ground surface as it was not possible to cover all the areas of venting in detail on every day. As the number of vents increased new areas needed to be delineated and the total area needing to be covered became larger. Also the daily surveys were only backed up by continuous flux measurements on two of the vents for a limited period of time so temporal variability is not well constrained.

An estimate was made of the total escape of CO_2 to the atmosphere during the experiment based on the averaged daily survey measurements and the areas covered. This gave a total figure of 40–70 kg during the measurement period, depending on the values chosen for the areas covered (the higher figure using the maximum ranges of x and y grid values, whereas the lower figure is an estimate of the actual area covered). This represents less than 5% of the injected CO_2. The range of values is likely to be an underestimate because the highest flux rate areas were not necessarily covered fully when the boundaries of the elevated flux zones were being delineated. All vents were not covered every day and so data for an earlier day would need to be included in the estimates, however continuous data suggest that fluxes were increasing up to the end of injection. No attempt has been made to estimate the uncertainty of the total release figure because too many factors are poorly constrained.

The low level leakage near the injection point (i.e. the injection well toe), detected only with isotopic data, has to be of very limited scale. Even if it is assumed that all the recorded flux consisted of injected CO_2 and taking an average flux of 2 g m^{-2} d^{-1}, which is greater than the maximum flux recorded in the central area by continuous flux monitoring, and assuming that rate of escape occurred over the entire 40 × 45 m soil gas and flux grid, it would only

amount to a total CO_2 leakage of about 18 kg or 1% of the injected CO_2; based on these assumptions this value is almost certainly a large overestimate.

The relatively small proportion of the injected CO_2 seen to have vented to the atmosphere through the ground implies that the bulk of the gas was contained in the shallow aquifer with some perhaps retained in the vadose zone. The hydrogeochemical data and the geophysical monitoring are consistent with free gas in the early stages of the injection followed by dissolution of the CO_2 in the ground water (Barrio et al., in press; Gal et al., 2013).

The shallow experiment at the CO_2 Field Lab has highlighted the difficulty of predicting the occurrence of surface leakage even from a relatively shallow injection depth of 20 m. This makes the location of fixed continuous monitoring equipment problematic as leakage may occur outside the pre-defined monitoring zone. The leakage was detected during the course of the experiment by the surface gas measurements, which were not restricted to a fixed central sampling zone and covered a larger area. They also had the flexibility to include additional measurements to delineate the areas of leakage and monitor the flux rates and it was possible to move some of the continuous monitoring equipment to more precisely define the leakage rates over time.

The difficulty of predicting where leakage might occur needs to be taken into account when designing baseline surveys, to ensure that areal coverage is adequate to provide a comparison with any suspected subsequent leakage and to allow criteria to be developed to act as a trigger for further investigations that might be required to establish the source of higher levels of CO_2 or other monitored gases.

Some clear indications of leakage were also detected by changes in water chemistry, which could be directly linked to increased CO_2 content (Gal et al., 2013). There were also responses in geophysical methods (EM, electrical logging, GPR) but some of these were difficult to interpret and these methods could not detect any effects due to CO_2 injection below the freshwater-saline water interface at a depth of 12–15 m (Barrio et al., in press).

Atmospheric monitoring was compromised by the escape of CO_2 directly to the atmosphere at the head of the injection well. This made it hard to distinguish whether any responses were from this source or from nearby areas of gas seepage through the ground. In addition 1 Hz averaged EC data show clear non-leakage inputs of CO_2 that occurred prior to injection. These could have been from vehicle movements or generators needed to power other monitoring equipment, even though efforts were made to site these as far from the experimental area as possible. Alternatively, they could have come from more distant sources, perhaps associated with the active gravel workings, or from road vehicles. The nearest road is only about 50 m from the site, albeit behind a ridge of sand and gravel.

Taken as a whole the monitoring datasets suggest a complex and tortuous migration of CO_2 laterally from the injection point, with dissolution, displacement of both saline and fresh groundwater, and then movement east and north out of the central most heavily monitored zone. The complexity of the migration paths is consistent with the highly variable nature of the deposits, which have a wide range of grain sizes and a mix of channelling, cross bedding and normal bedding. This behaviour was not predicted by pre-injection modelling, which suggested surface leakage more directly above the injection point (Bakk et al., 2012; Barrio et al., in press).

The site was disturbed by the drilling of the injection and monitoring wells and by the large amounts of water used for these operations and for subsequent testing. Ideally there would have been time to allow the site to re-equilibrate after these perturbations and to ensure that this had occurred through a longer period of baseline measurements. It appears that the cementing of the plastic casing of the well (necessary to allow certain types of geophysical measurements to be made) was not perfect, allowing CO_2 to escape initially along pathways close to the line of the well bore. Later, when the injection rate was increased, the gas exploited new migration paths to reach the surface further to the north in a general updip direction.

Zones of higher permeability were apparent around the four 20 m deep ERT (ALERT) arrays, where sediment had not completely collapsed around the electrode arrays on removal of the well casing, and other central monitoring wells. It was easy to insert soil gas probes here and voids could be discerned when this was done. Subsequent to the experiment some consolidation of the sediments occurred leading to surface depressions around some of the well heads. The CO_2 did not exploit these higher permeability zones, even though it was detected in water sampling along the ALERT wells (Gal et al., 2013), because bentonite seals had been emplaced at 20, 12 and c. 7 m below ground level around each of the arrays to prevent this and to isolate the water sampling points at 5, 10 and 15 m depth.

6. Conclusions

The shallow experiment at Svelvik has highlighted the difficulty in predicting the migration pathways and ultimate surface leakage of CO_2 even when the leakage is from a known injection point at shallow depth (20 m). In this case the CO_2 reached the surface at a number of locations between about 15 and 40 m horizontally from the injection point. This unpredictability makes the siting of fixed monitoring equipment problematic; although the aim may be to monitor a potential pathway for fluid migration, such as a well or a fault, seepage at surface may not necessarily occur close to the wellhead or at a particular point along a fault.

Initially the leaking CO_2 exploited a pathway close to the line of the injection well implying imperfect cementation around the plastic casing. As the injection rate was increased the gas followed additional pathways to emerge further north. The main areas of surface leakage were well defined by soil gas and flux measurements with subsurface hydrochemistry and geophysical methods giving some indications of the behaviour of the injected CO_2 below ground but not sufficient to delineate the plume in detail.

There are advantages in mobile approaches to monitoring, techniques which allow a relatively large area to be covered or those where fixed equipment can be moved to monitor at a new location. Thus in the case of the CO_2 Field Lab shallow experiment the wider area covered by soil gas and flux measurements enabled leakage to surface outside the predicted zone to be detected. This should also have been possible with mobile measuring methods had it been practicable to deploy these more extensively at the site (their use being largely ruled out by the plethora of surface equipment and personnel in a small area).

The individual areas of surface seepage of CO_2 were small (<10 m across, although some did coalesce), thus representing a small target to locate in the potentially large area covered by the surface footprint of an industrial scale CCS site. This is consistent with observations at other shallow surface release experiments (e.g. Lewicki et al., 2009; Strazisar et al., 2009) and at sites of natural CO_2 leakage (e.g. Annunziatellis et al., 2008; Beaubien et al., 2008; Jones et al., 2009; Krüger et al., 2011; Lewicki et al., 2007; Pettinelli et al., 2010; Rogie et al., 2000; Vodnik et al., 2006; Ziogou et al., 2013) where the surface expression and flux rates are similar.

Whilst it appears that the main areas of CO_2 degassing were identified, C and O isotopic data at a single point suggested a small amount of leaking injected gas closer to the injection point. This was not detectable in the soil gas concentrations or fluxes in spite of the low baseline values at the site, probably because the background

Table 2
Summary of the pros and cons of the different near surface gas techniques used for the CO_2 Field Lab project and their outcomes during the shallow injection experiment. Note that the costs are only relative between these methods.

Technique	Area	Mode	Pros	Cons	Outcomes at CO_2 Field Lab
Soil gas-field	Point	Survey	Quick and easy. Instant data. Relatively low cost	Low precision. Large areas time consuming so costs increase	Discovered/verified seeps over time
Soil gas-field lab	Point	Survey	Higher precision, data available in the field	More laborious and costly. Some delay in data. Large areas time consuming	Confirmation of field measurements at better precision
Soil gas lab	Point	Survey	Highest precision. Potential to analyse wider range of gases to determine source	Most laborious and costly. Data delayed. Large areas time consuming	Confirmation of field measurements
Soil gas monitoring probe(s)	Point(s)	Continuous	Relatively low cost continuous data at a network of points. Remote data access possible	Precision depends on sensors. Fixed points so could miss leakage (although easy to relocate)	No signs of leakage detected above injection point. Could have been redeployed to vents
C/O Isotopes – field	Point(s)	Continuous	Data available rapidly in field. May be able to determine source of gas if isotopic signatures diagnostic	Moderately high cost. May not be diagnostic of source in some cases. Single points only	Very sensitive to small amounts of leakage
C/O Isotopes – lab	Point	Survey	May be able to determine source of gas if isotopic signatures diagnostic	Higher cost. Delay in data. May not be diagnostic of source in some cases	Baseline data and confirmation of field results
Chamber flux	Small area (e.g. 0.03 m^2)	Survey	Quick and easy. Instant data. Relatively low cost	Coverage of large areas time consuming so costs increase	Discovered/verified seeps over time
Multichamber flux	Small areas ($n \times 0.03$ m^2)	Continuous	Moderate cost continuous data at a network of points. Remote data access possible	Fixed points so could miss leakage (although easy to relocate)	No leakage detected above injection point. Showed temporal changes of vents
Eddy covariance	Medium area (100 s m^2)	Continuous	Flux over larger area, useful additional parameters for general data interpretation. Continuous data at high rate	Footprint varies with wind speed and direction. Assumptions implicit in method may not be met. Susceptible to CO_2 inputs other than leakage. Complex data processing	Leakage not detected because of distance and wind direction and speed. Affected by above ground releases and other sources of CO_2
Mobile open path laser	Large areas (km^2)	Survey	Coverage of large areas quickly with instant data at high repeat rates - can check anomalies immediately	Needs vehicle access. Tall vegetation and vehicle exhaust may affect readings. Moderately high cost	Restricted by crowded site. May have detected leakage but affected by above ground release
Weather station	Point	Continuous	Very useful adjunct for data interpretation if data not available from nearby existing weather station	Additional cost	Useful background information to aid interpretation

levels above the injection point were generally falling during injection. It is possible that such low level leakage was more widespread, although not likely to have been responsible for the escape of a significant amount of the injected gas at Svelvik. However, this raises the possibility that low level seepage could be more widespread than is currently thought as attention is inevitably focussed on the more obvious vent features, which are easily detectable above background levels. That said, this process may also be very site specific, with the highly permeable nature of the sediments at Svelvik contributing to it. The extent of low level gas egress could be tested at natural CO_2 seepage sites using, for example, stable C isotope ratios. This is feasible because at many sites there is a sufficient contrast between the isotopic signature of the escaping geogenic CO_2 and that produced by shallow biological processes to make this a more sensitive leakage indicator than soil gas CO_2 concentrations or fluxes. This would help to establish whether leakage is mainly through relatively small discrete vents with high concentrations and fluxes or if there is a significant component emitted at much lower rates but potentially over larger areas. This is an important consideration in the quantification of any detected leakage as required by EU Emissions trading legislation (European Union, 2009a).

The relative pros and cons of the of the different near surface gas techniques, and associated methods, used at the CO_2 Field Lab have been summarised in Table 2. The table also provides an assessment of the outcomes of their use during the shallow injection experiment.

References

Annunziatellis, A., Beaubien, S.E., Bigi, S., Ciotoli, G., Coltella, M., Lombardi, S., 2008. Gas migration along fault systems and through the vadose zone in the Latera caldera (central Italy): implications for CO_2 geological storage. Int. J. Greenh. Gas Control 2, 353–372.

Bakk, A., Girard, J.-F., Lindeberg, E., Aker, E., Wertz, F., Buddensiek, M., Barrio, M., Jones, D., 2012. CO_2 Field Lab at Svelvik Ridge: site suitability. Energy Procedia 23, 306–312.

Barrio, M., Bakk, A., Grimstad, A.-A., Querendez, E., Jones, D.G., Kuras, O., Gal, F., Girard, J.-F., Pezard, P., Depraz, L., Baudin, E., Børresen, M.H., Sønneland, L., in press. CO_2 migration monitoring methodology in the shallow subsurface: lessons learned from the CO_2 Field Lab project. Energy Procedia.

Beaubien, S.E., Ciotoli, G., Coombs, P., Dictor, M.C., Krüger, M., Lombardi, S., Pearce, J.M., West, J.M., 2008. The impact of a naturally occurring CO_2 gas vent on the shallow ecosystem and soil chemistry of a Mediterranean pasture (Latera, Italy). Int. J. Greenh. Gas Control 2, 373–387.

Beaubien, S.E., Jones, D.G., Gal, F., Barkwith, A.K.A.P., Braibant, G., Baubron, J.C., Ciotoli, G., Graziani, S., Lister, T.R., Lombardi, S., Michel, K., Quattrocchi, F., Strutt, M.H., 2013. Monitoring of near-surface gas geochemistry at the Weyburn, Canada, CO_2-EOR site, 2001–2011. Int. J. Greenh. Gas Control 16 (Suppl. 1), S236–S262.

Deines, P., 1980. The isotopic composition of reduced organic carbon. In: Fritz, P., Fontes, J.C. (Eds.), Handbook of Environmental Isotope Geochemistry 1. The Terrestrial Environment. Elsevier, Amsterdam, pp. 329–406.

Dillen, M., Lindeberg, E., Aagaard, P., Aker, E., Sæther, O.M., Johansen, H., Lien, M., Hatzignatiou, D.G., Golmen, L., Hellevang, J., 2009. A field laboratory for monitoring CO_2 leakage. Energy Procedia 1, 2397–2404.

Edinburgh University, 2011. EdiRe.

European Union, 2009a. Directive 2009/29/EC of the European Parliament and of the Council of 23 April 2009 amending Directive 2003/87/EC so as to improve and extend the greenhouse gas emission allowance trading scheme of the Community (Text with EEA relevance).

European Union, 2009b. Directive 2009/31/EC of the European Parliament and of the Council of 23 April 2009 on the geological storage of carbon dioxide and amending Council Directive 85/337/EEC, European Parliament and Council Directives 2000/60/EC, 2001/80/EC, 2004/35/EC, 2006/12/EC, 2008/1/EC and Regulation (EC) No 1013/2006 (Text with EEA relevance).

Farquhar, G.D., Lloyd, J., Taylor, J.A., Flanagan, L.B., Syvertsen, J.P., Hubick, K.T., Wong, S.C., Ehleringer, J.R., 1993. Vegetation effects on the isotope composition of oxygen in atmospheric CO_2. Nature 363, 439–443.

Fessenden, J.E., Clegg, S.M., Rahn, T.A., Humphries, S.D., Baldridge, W.S., 2010. Novel MVA tools to track CO_2 seepage, tested at the ZERT controlled release site in Bozeman, MT. Environ. Earth Sci. 60, 325–334.

Gal, F., Proust, E., Humez, P., Braibant, G., Brach, M., Koch, F., Widory, D., Girard, J.-F., 2013. Inducing a CO2 leak into a shallow Aquifer (CO_2 Field Lab Eurogia+Project): monitoring the CO_2 Plume in ground waters. Energy Procedia 37, 3583–3593.

Gilfillan, S., Haszeldine, S., 2011. Report on Noble Gas, Carbon Stable Isotope and HCO_3, The Kerr Investigation. IPAC CO2 Research Incorporated.

Hinkle, M.E., 1994. Environmental-conditions affecting concentrations of He, CO_2, O_2 and N_2 in soil gases. Appl. Geochem. 9, 53–63.

Hofmann, M.E.G., Horváth, B., Pack, A., 2012. Triple oxygen isotope equilibrium fractionation between carbon dioxide and water. Earth Planet. Sci. Lett. 319–320, 159–164.

International Energy Agency, 2009. Technology Roadmap: Carbon Capture and Storage. International Energy Agency, Paris, pp. 46.

Jones, D.G., Barlow, T., Beaubien, S.E., Ciotoli, G., Lister, T.R., Lombardi, S., May, F., Möller, I., Pearce, J.M., Shaw, R.A., 2009. New and established techniques for surface gas monitoring at onshore CO_2 storage sites. Energy Procedia 1, 2127–2134.

Krevor, S., Perrin, J.-C., Esposito, A., Rella, C., Benson, S., 2010. Rapid detection and characterization of surface CO_2 leakage through the real-time measurement of $\delta^{13}C$ signatures in CO_2 flux from the ground. Int. J. Greenh. Gas Control 4, 811–815.

Krüger, M., Jones, D., Frerichs, J., Oppermann, B.I., West, J., Coombs, P., Green, K., Barlow, T., Lister, R., Shaw, R., Strutt, M., Möller, I., 2011. Effects of elevated CO_2 concentrations on the vegetation and microbial populations at a terrestrial CO_2 vent at Laacher See, Germany. Int. J. Greenh. Gas Control 5, 1093–1098.

Lewicki, J., Birkholzer, J., Tsang, C.-F., 2007. Natural and industrial analogues for leakage of CO_2 from storage reservoirs: identification of features, events, and processes and lessons learned. Environ. Geol. 52, 457–467.

Lewicki, J.L., Hilley, G.E., Fischer, M.L., Pana, L., Oldenburg, C.M., Dobeck, L., Spangler, L., 2009. Detection of CO_2 leakage by eddy covariance during the ZERT project's CO_2 release experiments. Energy Procedia 1, 2301–2306.

Lombardi, S., Annunziatellis, A., Beaubien, S.E., Ciotoli, G., Coltella, M., 2008. Natural analogues and test sites for CO_2 geological sequestration: experience at Latera, Italy. First Break 26, 39–43.

McAlexander, I., Rau, G.H., Liem, J., Owano, T., Fellers, R., Baer, D., Gupta, M., 2011. Deployment of a carbon isotope ratiometer for the monitoring of CO_2 sequestration leakage. Anal. Chem. 83, 6223–6229.

Moni, C., Rasse, D.P., 2013. Simulated CO_2 leakage experiment in terrestrial environment: monitoring and detecting the effect on a cover crop using ^{13}C analysis. Energy Procedia 37, 3479–3485.

Pettinelli, E., Beaubien, S.E., Zaja, A., Menghini, A., Praticelli, N., Mattei, E., Di Matteo, A., Annunziatellis, A., Ciotoli, G., Lombardi, S., 2010. Characterization of a gas vent using various geophysical and geochemical methods. Geophysics 75, B137–B146.

Risk, D., McArthur, G., Nickerson, N., Phillips, C., Hart, C., Egan, J., Lavoie, M., 2013. Bulk and isotopic characterization of biogenic CO_2 sources and variability in the Weyburn injection area. Int. J. Greenh. Gas Control 16 (Suppl. 1), S263–S275.

Rogie, J.D., Kerrick, D.M., Chiodini, G., Frondini, F., 2000. Flux measurements of non-volcanic CO_2 emission from some vents in Central Italy. J. Geophys. Res.-Solid Earth 105, 8435–8445.

Romanak, K., Sherk, G.W., Hovorka, S., Yang, C., 2013. Assessment of alleged CO_2 leakage at the Kerr Farm using a simple process-based soil gas technique: implications for carbon capture, utilization, and storage (CCUS) monitoring. Energy Procedia 37, 4242–4248.

Romanak, K.D., Bennett, P.C., Yang, C., Hovorka, S.D., 2012. Process-based approach to CO_2 leakage detection by vadose zone gas monitoring at geologic CO_2 storage sites. Geophys. Res. Lett. 39, L15405.

Sørensen, R., 1981. Foreløpig beskrivelse til kvartærgeologisk kart SVELVIK – CL 083, M1:10 000. Norges geologiske undersøkelse.

Strazisar, B.R., Wells, A.W., Diehl, J.R., Hammack, R.W., Veloski, G.A., 2009. Near-surface monitoring for the ZERT shallow CO_2 injection project. Int. J. Greenh. Gas Control 3, 736–744.

Trium, 2011. Site Assessment (SW-30-05-13-W2M), Weyburn, Saskatchewan, p. 50.

Vodnik, D., Kastelec, D., Pfanz, H., Macek, I., Turk, B., 2006. Small-scale spatial variation in soil CO_2 concentration in a natural carbon dioxide spring and some related plant responses. Geoderma 133, 309–319.

Ziogou, F., Gemeni, V., Koukouzas, N., de Angelis, D., Libertini, S., Beaubien, S.E., Lombardi, S., West, J.M., Jones, D.G., Coombs, P., Barlow, T.S., Gwosdz, S., Krüger, M., 2013. Potential environmental impacts of CO_2 leakage from the study of natural analogue sites in Europe. Energy Procedia 37, 3521–3528.